Automating Proliferation Rate Estimation from Breast Cancer Ki-67 Histology Images

Heba Z. Al-Lahham[b], Raja S Alomari[a,b], Hazem Hiary[b], and Vipin Chaudhary[a]
[a]University At Buffalo, SUNY, Buffalo, NY 14260
[b]The University of Jordan, Amman, Jordan 11942

ABSTRACT

Breast cancer is the second cause of women death and the most diagnosed female cancer in the US. Proliferation rate estimation (PRE) is one of the prognostic indicators that guide the treatment protocols and it is clinically performed from Ki-67 histopathology images. Automating PRE substantially increases the efficiency of the pathologists. Moreover, presenting a deterministic and reproducible proliferation rate value is crucial to reduce inter-observer variability. To that end, we propose a fully automated CAD system for PRE from the Ki-67 histopathology images. This CAD system is based on a model of three steps: image pre-processing, image clustering, and nuclei segmentation and counting that are finally followed by PRE. The first step is based on customized color modification and color-space transformation. Then, image pixels are clustered by K-Means depending on the features extracted from the images derived from the first step. Finally, nuclei are segmented and counted using global thresholding, mathematical morphology and connected component analysis. Our experimental results on fifty Ki-67-stained histopathology images show a significant agreement between our CAD's automated PRE and the gold standard's one, where the latter is an average between two observers' estimates. The Paired T-Test, for the automated and manual estimates, shows ρ = 0.86, 0.45, 0.8 for the brown nuclei count, blue nuclei count, and proliferation rate, respectively. Thus, our proposed CAD system is as reliable as the pathologist estimating the proliferation rate. Yet, its estimate is reproducible.

Keywords: Ki-67,Nuclei Counting, Proliferation Rate, Breast Cancer, Digital Histopathology.

1. INTRODUCTION

Breast cancer is the most common female cancer in the US, the second most common cause of cancer death in women ages 20 to 59, and the main cause of death in women ages 40 to 59. It was reported that the probability of developing invasive breast cancer within ages 40 to 59 and 60 to 69 was 3.75% and 3.45%, respectively, from 2005 to 2007. Moreover, from all new cancer cases among women it alone was expected to account for 28% in 2010 and 30% in 2011.[1,2]

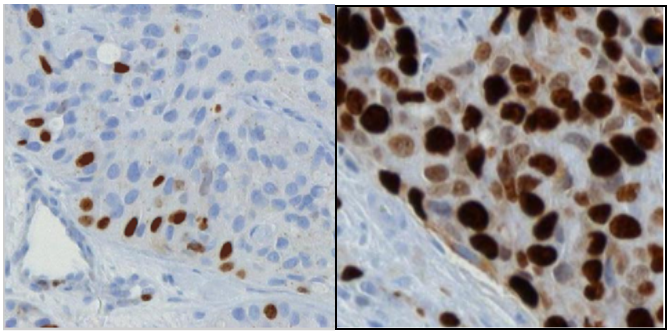

Figure 1: Sample Ki-67 stained histology images

The diagnostic evaluation of a patient with suspected breast cancer includes screening, diagnostic breast imaging, and breast biopsy [3]. A patient with a suspicious pre-screening urges the pathologist for taking a breast biopsy, which is then treated and sliced on lab slides. Since the digital histopathology emerged, these slides are scanned using high resolution scanners allowing the resulting high resolution image (40X) to be communicated instead of the physical slide. By examining these high resolution images of the biopsy, the pathologist diagnoses the cancer and presents various measurements for cancer grading and, in some clinical standard, presents the prognosis for the cancer.

The measurement of proliferation rate can be used in conjunction with other measurements as a prognostic indicator which guides the treatment protocols in the clinical practice.[4] The cancer cells are known to be in the growing and dividing phase and the proliferation rate is measured depending on finding out the percentage of cancer cells count over the whole cells count.[5,6] Some techniques developed to measure the proliferation rate are: Mitotic index, S-phase fraction, Nuclear antigen ImmunoHistoChemistry (IHC) including Ki-67 and PCNA-staining Cyclins and PET.[4] These techniques have their own advantages and disadvantages based on the experimental lab work. Comparing with other

Medical Imaging 2012: Computer-Aided Diagnosis, edited by Bram van Ginneken, Carol L. Novak,
Proc. of SPIE Vol. 8315, 83152A · © 2012 SPIE · CCC code: 1605-7422/12/$18 · doi: 10.1117/12.911009

markers, Ki-67 staining was stated to have many advantages: being easy to perform, sensitive antibodies anduses a small amount of tissue. The disadvantage of nuclei counting over the Ki-67 stained tissue is the time consumption.[4,5] This disadvantage makes the process of estimating the proliferation rate a highly subjective one, since the pathologist looks quickly at the image and gives an approximate nuclei count and proliferation rate as well.

In Ki-67 stained histopathology images, cells that show brown or yellow staining are scored as positive, while the blue ones are scored as negative, as shown in Figure 1. The proliferation rate assessed using Ki-67 is evaluated as the percentage of the total number of tumor positive cells; which equates the growth fraction of the tumor.[4,6]Accurately automating the process of nuclei counting and evaluating the proliferation rate from the Ki-67 images has many advantages, since it would: (1) utilize the pathologist time that is consumed in manual nuclei counting; (2) serve as a second opinion; and (3) help in gaining a more deterministic decision in the treatment plan.

Recent research has been focusing on building automated CAD systems for various cancer types in the human body to lend hands in cancer different diagnosing and prognosing routines. These automated systems were not meant to replace the radiologist or pathologist, but to support as a second opinion. “Second opinion” means that the analysis results from these systems will be considered for its advantages of speed, accuracy, reproducibility and effort saving, but the final decision and recommendations will be human-driven. Breast cancer detection [7], grading [8], and growth-rate estimation [9] are some clinical routines in which automated computer-aided systems are used to help in defining the degree of the disease severity and guiding the treatment protocols.

Variety of imaging modalities is used in cancer clinics; such as: mammography, ultrasound, Magnetic Resonance Imaging (MRI), Computed Tomography (CT), digital mammography[10,11]and histology images[8,9]. Regardless of these types of cancer images, the automated CAD systems follow some general approach to analyze such images, which may vary depending on the system purpose and the used images. This general approach may involve, but not strictly, these steps: image pre-processing, image segmentation, feature extraction and selection, and classification.[10,12,13] Image pre-processing techniques in such CAD systems are used for image de-noising and color-space transformations.[12,14,15] Image segmentation partitions the image into non-overlapping, constituent regions which are homogeneous with respect to some characteristic such as intensity or texture. Methods for performing segmentations in these systems vary widely depending on the purpose, imaging modality, and other factors. Thus, there is no universal method to carry out adequate segmentation method that yields acceptable results for every medical image.[10] Some of the used segmentation methods for medical images are: Local and global adaptive thresholding[18], region growing, Markov random field (MRF),[10,16,17] morphological operations, marker controlled watershed[16,18,19], second-order edge [9], and active contours[10,20]. Some other classification and clustering approaches are also used in medical image segmentation, such as: Artificial Neural Networks (ANN)[16,21], Kohenen Self-Organizing Map (SOM)[22], Support Vector Machines (SVM)[10,16,17], K Nearest Neighbor (KNN)[19], and K-Means[23]. The region of interest (ROI) resulting from the segmentation are allocated for feature extraction and selection. CIELab color-space and Discrete Wavelet Transformation (DWT) could be used in feature and texture extraction in some CAD systems[14,19,22], while Principle Component Analysis (PCA) is used to reduce the dimensionality of features[9].

Some efforts have been performed in the literature for Nuclei counting. Phukpattaranont, et al. [14] developed a system for analyzing microscopic images for nuclear stained breast cancer cell counting. They used NN and mathematical morphology to segment cells, while they used CIELab values, circularity ratio, and area for feature extraction. Then, the classification task was performed using the Euclidean Distance (ED) of selected features. Kothari et al. [15] presented a semi-automatic method for cell segmentation and counting from digital tissue images. Phukpattaranont and Boonyaphiphat[18]built their automatic cell counting system for microscopic breast cancer tissue images. They removed the noise depending on CIELab and anisotropic diffusion filtering. Then,they segmentedcells using local adaptive thresholding, morphological operations, and cell size considerations followed by marker-controlled watershed. Loukas et al. [9] presented their approach for automated counting of cancer cell nuclei in tissue sections. They worked on analyzing histological sections from different squamous cell cancers stained for proliferation using Ki-67 and cyclin A detection. The overall number of cells was detected, using second-order edge detection methodology. Then proliferating cells were located using principal component analysis (PCA) of the image, combined with histogram thresholding.

In this paper, we propose a CAD system that analyzes the Ki-67 images to automate nuclei counting and proliferation rate evaluating as well. This model uses K-Means to classify the nuclei into positive and negative. This classification depends mainly on the features extracted from the *L*a*b** color-space model of the Ki-67 images. Some pre- and post-processing is done to enhance the overall automating process. We study the performance of accurately automating the process of proliferation rate evaluation over the manual process.

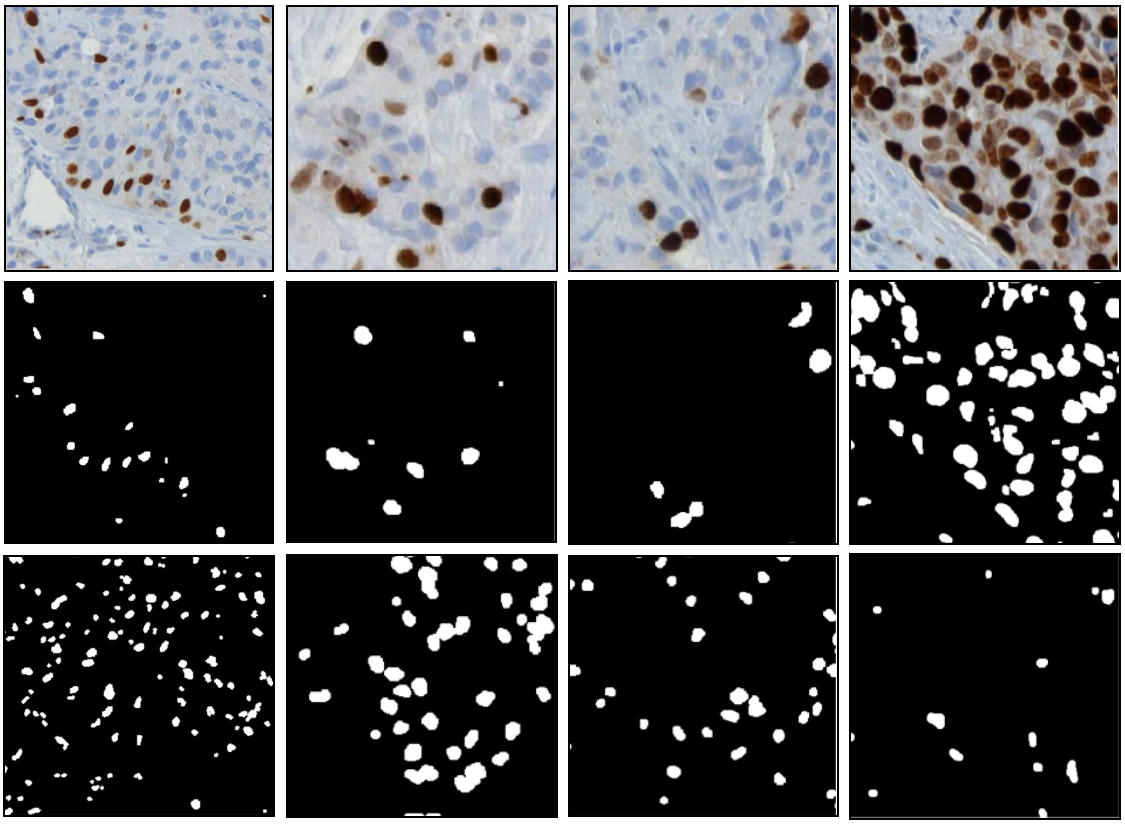

Figure 2. (First row) The Ki-67-Stained Histology, where the brown nuclei are positive cells, while the blue nuclei are negatives. (Second row) The corresponding segmented brown nuclei. (Third row) The corresponding segmented blue nuclei.

2. OUR PROPOSED CAD

We propose a CAD system that analyzes the Ki-67 images to automate nuclei counting and PRE. This CADworks to classify the nuclei into brown and blue ones using K-means clustering. This clustering depends on the features extracted from the *L*a*b** color-space model of the Ki-67 images. These features are: 1) The *a** channel, 2) The *b** channel.

As shown in Figure 3, the procedure of our approach is composed of three stages followed by PRE out of the resulting nuclei count; 1) image pre-processing, 2) image clustering 3) nuclei segmentation and counting. Image pre-processing stage consists of customized color modification and color space transformation. Image clustering stage consists of clustering the image into three regions using K-Means and pixel labeling. Nuclei segmentation and counting stage comprises global thresholding, mathematical morphology and connected objects count. Details of each step are as follows:

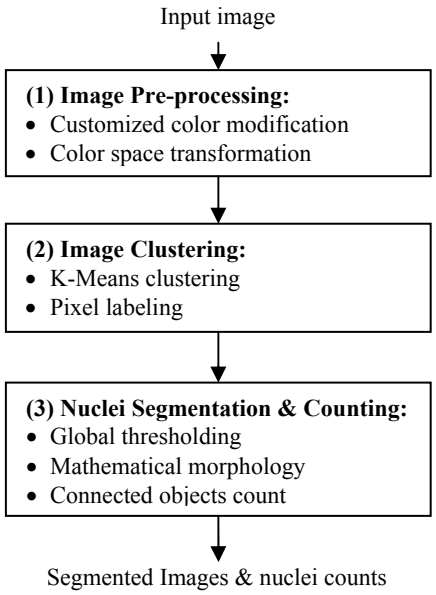

Figure 3 The stages of the nuclei counting algorithm

2.1 Image pre-processing

Firstly, we do a customized color modification over the pixels of the dark brown nuclei parts that are less than specific values in the three channels of the RGB color model image. The need for this modification was figured out experimentally to ensure clustering these parts with the brown nuclei.

Secondly, we use color space transformation to convert the original images from RGB color model into *L*a*b** color-space. That's due to considering the *L*a*b* as an excellent decoupler of intensity and color represented by *a** and *b**, which makes it useful in both image manipulation and image compression applications. The *L*a*b* space can be defined by: [23]

$$L^* = 116 \cdot \left(\frac{Y}{Yw}\right)^{\frac{1}{3}} - 16 \quad (1)$$

$$a^* = 500\left[\left(\frac{X}{Xw}\right)^{\frac{1}{3}} - \left(\frac{Y}{Yw}\right)^{\frac{1}{3}}\right] \quad (2)$$

$$\mathrm{b}^* = 200\left[\left(\frac{\mathrm{Y}}{\mathrm{Yw}}\right)^{\frac{1}{3}} - \left(\frac{\mathrm{Z}}{\mathrm{Zw}}\right)^{\frac{1}{3}}\right] \quad (3)$$

where X/Xw, Y/Yw, Z/Zw> 0.01. The values Xw, Yw, Zw are the CIE tristimulus values of the reference white under the reference illumination, and X, Y, Z are the tristimulus values, which are mapped to the CIE color space. While the *L** component represents intensity, *a** and *b** components are proportional to red-green and yellow-blue color contents, respectively.

2.2 Image clustering

In this stage, using K-Means algorithm[24,25], the image is clustered into three regions: the brown nuclei, the blue nuclei and the remaining tissue. K-means is an unsupervised technique that works as an intensity-based classifier for the image pixels over the extracted features, *a*b**.We set the number of clusters (K) tothree in order to handle the three regions. K-Means algorithm minimizes the intra-cluster variation iteratively. The unlabelled pixels are assigned to the nearest clusters based on their distances to the initial cluster centroids, then the cluster centroid is updated and the pixels are re-assigned. Our K-Means algorithm terminates after three iterations.Then, the resulting clustered pixels are labeled using cluster-based labels. This helps in isolating the brown-nuclei-labeled and blue-nuclei-labeled clustered regions into separate images for further processing.

2.3 Nuclei segmentation and counting

We use a combination of global thresholding, morphological operations, and connectedcomponent count in our counting algorithm. For Global thresholding, we apply a global thresholding, using Otsu's method, for each brown-labeled and blue-labeled image, separately.[26] This thresholding method chooses the suitable threshold that minimizes the intra-class variance of the binary images that result from this step. Then, we process the resulting binary images using morphological opening[27], which eliminates spike noise and fills holes as shown in Figure 2 (second and third rows). After that, we count the connected components in the brown-segmented image that represents the brown nuclei count, while the connected objects count in the blue-segmented image represents the blue nuclei count.

Finally, we evaluate the proliferation rateby dividing the resulting brown nuclei count by the total nuclei count (*i.e.*the sum of brown and blue nuclei). We verify the accuracy of the results compared to the gold standard values estimated manually by two observers. These values are the manual count of the brown and the blue nuclei, and the evaluated proliferation rate. Then we study the performance of accurately automating the process of proliferation rate evaluation by our proposed model over the manual process. This is the major experimental setting that proves the robustness and reliability of the proposed model.

3. DATA AND EXPERIMENTAL RESULTS

Our data is contains fifty Ki-67 stained histopathology digital images of breast cancer. Positive cells have a brown color, whereas negative cells have a blue color. Each digital image comes with the tumor count scores from two independent observers: one expert pathologist and one student trained on this counting. We consider the average count among the observers' readings as our gold standard for nuclei counting. Both observers' estimates are not typically equal; this is due to the fact that perceiving a staining nucleus depends on one's subjective awareness. Figure 4 and Figure 5 show that the relation between first and second observers' nuclei count estimates can be considered as a linear relationship, though there still some variation from each other.To that end; we investigate how close our CAD estimates are from the average estimates and from each individual observer, as well.

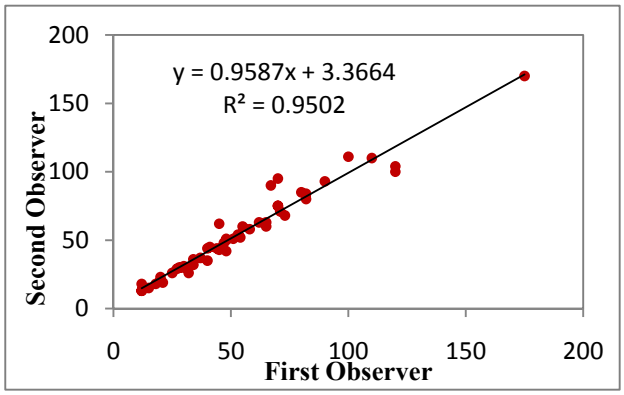

Figure 4: Relationship between first and second observers' nuclei count estimates in brown nuclei.

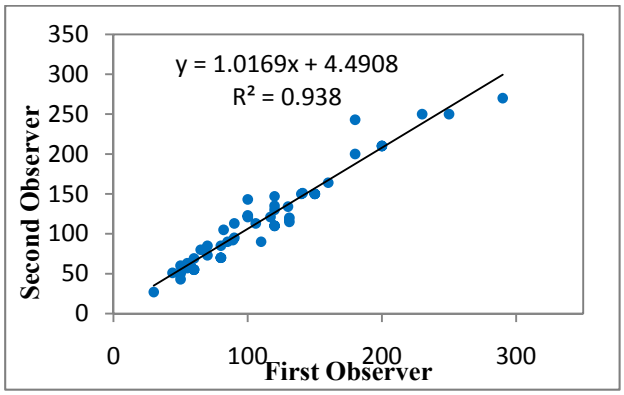

Figure 5: Relationship between first and second observers' nuclei count estimates in blue nuclei

We intended not only to report the estimated proliferation rate, but also the brown and blue nuclei count. This is for accuracy purposes since the proliferation rate depends on both, the brown and blue nuclei count. We calculate the percentage difference in nuclei counting and the actual difference in PRE between manually and automatically estimated values. Figure 6 shows the differences represented as the Y-axis, while the X-axis is the case identification number that runs between 1 up to 50. To further show the consistency of our results, Table 1 presents also the average percentage difference for each 10 cases (selected randomly and disjointly) of the fifty cases. This table gives a good sense about the consistency in the differences besides the Paired T-Test result.Next, to evaluate our automated model efficiency, we study the differences between manually and automatically estimated values, by applying the Paired T-Test [28]:

$$\rho = \frac{x - y}{\sigma/\sqrt{n}} \tag{4}$$

where x and y are the mean value of the two samples, σ is the standard deviation of the differences between the two samples (X and Y), and n is the sample size. If the T-Test value was more than the significance level (0.05), the two samples are said to be statistically insignificant. Table 2 presents the significance values resulting from the Paired T-Test on the fifty samples. Since all the stated values between the automated estimates, on one hand,and the average and individual observers, on the other hand, are above the significance level value (0.05), it's obvious that all the estimated values over the specified pairs are statistically insignificant. Though, the significance values between the individual observers' estimates show significance in blue nuclei count. Thus, our proposed K-Means-based model could be considered as reliable as the individual experts and the average expert as well.

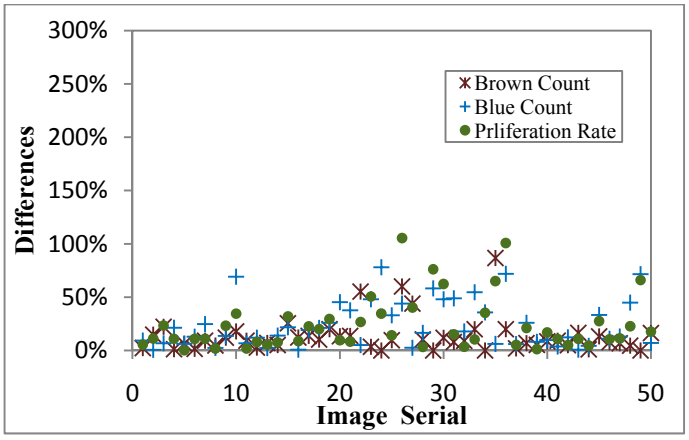

Figure 6 Differences between automated and gold standard estimates in Brown and Blue nuclei counting and PRE for each of the fifty cases to show the consistency in our results.

Table 1: Average Percentage Difference.

Image Set	Percentage Difference		
	Brown Count	Blue Count	Proliferation Rate
1-10	9%	17%	13%
11-20	12%	17%	15%
21-30	21%	47%	42%
31-40	17%	28%	27%
41-50	8%	20%	29%
Average	**13%**	**26%**	**25%**

Table 2): Significance Values Resulting from the Paired T-Test

Pairs	Significance Values (ρ)		
	Brown Count	Blue Count	Proliferation Rate
Observer1- Observer2	0.27	< 0.05	0.34
Automated-Observer1	0.62	0.19	0.96
Automated-Observer2	0.69	0.97	0.83
Automated-Average	0.86	0.45	0.8

4. CONCLUSION

We proposed a CAD systemfor automatic proliferation rate estimation from the Ki-67 histology digital images of breast cancer. We did color transformation from RGB color model to the *L*a*b** one. Then, we used K-Means to cluster the image pixels over the extracted features (*a*b**) form the image. After that, we used the global thresholding, mathematical morphology and connected objects count to segment the brown and blue nuclei, count them and evaluate the proliferation rate. We tested our model on fifty cases and calculated the average differences between the manually and automatically estimated values. The average percentage difference of the brown nuclei, blue nuclei count and evaluated proliferation rate were 13%, 26% and 25%, respectively. We studied the statistical significance of the difference values and found $\rho = 0.86, 0.45, 0.8$ for brown nuclei count, blue nuclei count and evaluated proliferation rate, respectively. This indicates statistical insignificance between the manual process and automated process. Hence, our CAD system produces proliferation rate estimate that is undistinguished from the expert pathologists. However, our automated estimate is reproducible and deterministic unlike manual estimates.

REFERENCES

[1] Jemal, A., et al., "Cancer statistics," CA Cancer J Clin. 60(5), 277–300 (2010).

[2] Siegel R, Ward E, Brawley O, and Jemal A, "Cancer statistics, 2011: the impact of eliminating socioeconomic and racial disparities on premature cancer deaths". CA: A Cancer Journal for Clinicians, 61(4), 212–236 (July/August 2011).

[3] Edge SB., et al., "AJCC cancer staging manual," New York: Springer. 7th edition. (2010)

[4] Beresford, MJ., Wilson, GD., and Makris, A., "Measuring proliferation in breast cancer: practicalities and applications," Breast Cancer Res. 8(6), 216 (2006).

[5] Urruticoechea, Ander, Smith, Ian E., and Dowsett, Mitch., "Proliferation Marker Ki-67 in Early Breast Cancer," Journal of Clinical Oncology. 23, 7212-7220 (2005).

[6] Klauber-DeMore, Nancy, et al., "Biological Behavior of Human Breast Cancer Micrometastases," Clinical Cancer Research. 7, 2434–2439 (August 2001).

[7] Sheshadri, HS., and Kandaswamy, A., "Computer aided decision system for early detection of breast cancer," Indian J. Med. Res. 124, 149-154 (2006).

[8] Doyle, S.,Agner, S., Madabhushi, A., Feldman, M., and Tomaszeweski, J., "Automated grading of breast cancer histopathology using spectral clustering with textural and architectural imagefeatures," Biomedical Imaging: from Nano to Macro. 496-499 (2008).

[9] Loukas, CG., Wilson, GD., Vojnovic, B., and Linney, A.,"An Image Analysis-Based Approach for Automated Counting of Cancer Cell Nuclei in Tissue Sections,"Cytometry. 55A(1), 30–42 (2003).

[10] Pham, DL.,Xu, C., and Prince, JL., "A survey of current methods in medical image segmentation,"Annual Review of Biomedical Engineering, Palo Alto. 315–337 (2000).

[11] Lord, SJ., Lei, W., Craft, P., et al., "A systematic review of the effectiveness of magnetic resonance imaging (MRI) as an addition to mammography and ultrasound in screening young women at high risk of breast cancer," Eur J Cancer. 43(13), 1905-1917 (2007).
[12] Cheng, HD., Shan, J., Ju, W., Guo, Y., and Zhang, L., "Automated breast cancer detection and classification using ultrasound images: A survey," Pattern Recognition. 43, 299-317 (2010).
[13] Olabarriaga, SD., and Smeulders, AWM., "Interaction in the segmentation of medical images: A survey," Medical Image Analysis. 5(2), 127–142 (2001).
[14] Phukpattaranont, P., Limsiroratana, S., andBoonyaphiphat, P.,"Computer-Aided System for Microscopic Images: Application to Breast Cancer Nuclei Counting," International Journal Of Applied Biomedical Engineering. 69-74 (2009).
[15] Kothari, S., Chaudry, Q., and Wang, M. D., "Automated cell counting and cluster segmentation using concavity detection and ellipse fitting techniques," IEEE International Symposium on Biomedical Imaging (ISBI'09). (2009)
[16] Kuo, Y., Ko, C., and Lai, J., "Automated Assessment in HER-2/neuImmunohistochemical Expression of Breast Cancer," International Symposium on Computer, Communication, Control and Automation (3CA). 2,585-588 (May 2010)
[17] Basavanhally, A. N., Ganesan, S., Agner, S., Monaco, J. P., Feldman, M. D., and Tomaszewski, J. E., et al., "Computerized Image-Based Detection and Grading of Lymphocytic Infiltration in HER2+ Breast Cancer Histopathology," 57(3), 642-653 (2010).
[18] Phukpattaranont, P., and Boonyaphiphat, P.,"An Automatic Cell Counting Method for a Microscopic Tissue Image from Breast Cancer," 3rd Kuala Lumpur International Conference on Biomedical Engineering 2006, Springer Berlin Heidelberg. 15(8), 241-244 (2007).
[19] Nandy, K., Gudla, P.R., Meaburn, K.J., Misteli, T., and Lockett, S.J., "Automatic nuclei segmentation and spatial FISH analysis for cancer detection," Engineering in Medicine and Biology Society, 2009. EMBC 2009. Annual International Conference of the IEEE. 6718-6721 (Sept. 2009).
[20] Street, W., Wolberg, W., andMangasarian, O., "Nuclear feature extraction for breast tumor diagnosis," IS&T/SPIE International Symposium on Electronic Imaging: Science and Technology. 1905, 861-870 (1993).
[21] Mao-jun, S., Zhao-bin, W., Hong-juan, Z., and Yi-de, M., "A New Method for Blood Cell Image Segmentation and Counting Based on PCNN and Autowave," Communications, Control and Signal Processing, 2008. ISCCSP 2008. 3rd International Symposium. 6-9 (March 2008).
[22] Zhang, J., Liu, Q. and Chen, Z., "A medical image segmentation method based on SOM and wavelet transforms," Journal of Communication and Computer. 2(5), 46-50 (2005).
[23] Gonzalez, Rafael C. and Woods, Richard E. [Digital Image Processing], Pearson Education, Inc., New Jersey, 3rd edition. 433-436 (2008).
[24] Likas, Aristidis, Vlassis, Nikos, Verbeek, and Jakob J., "The global k-means clustering algorithm," Pattern Recognition. 36(2), 451-461 (February 2003).
[25] Jain, A. K., Murty, M. N., and Flynn, P. J., "Data Clustering: A Review," ACM Comp. Surveys (CSUR). 31(3), 264-323 (1999).
[26] N. Otsu, "A threshold selection method from gray level histograms," IEEE Trans. Syst. Man Cybern. SMC-9, 62-66 (1979).
[27] Serra, J. (1982). Image Analysis and Mathematical Morphology, Academic Press, London.
[28] L. Wasserman, [All of Statistics: A Concise Course in Statist. Inference], Springer Texts in Stat., Springer, (2004).